Split Crystallization during Debranching of Maltodextrins at High Concentration by Isoamylase

A. Pohu,[†] V. Planchot,[†] J. L. Putaux,[‡] P. Colonna,[†] and A. Buléon*,[†]

INRA, Rue de la Géraudière, BP 71627, 44316 Nantes Cedex 3, France, and Centre de Recherches sur les Macromolécules Végétales (affiliated with the Joseph Fourier University of Grenoble), CNRS, BP 53, 38041 Grenoble cedex 9, France

Received February 25, 2004; Revised Manuscript Received May 10, 2004

Debranching and crystallization occurring during the enzymatic treatment of 25% (w/v) aqueous solutions of maltodextrins by isoamylase at 52 °C were studied. The morphology as well as the crystal and molecular structures of the precipitates formed at different stages of the reaction were characterized. Two types of resulting products, differing in terms of structure and morphology, were evidenced. A loose B-type network, containing linear and branched chains of highest molecular weight, was mainly formed during the first 12 h of reaction, whereas aggregates of A-type lamellar crystals, made of short linear chains, were predominantly obtained between 12 and 48 h. The aggregation behavior as a function of temperature and molecular weight distribution of such substrates was discussed and compared to that of related starch products.

1. Introduction

Aggregation and/or crystallization of polymers strongly depend on factors such as solvent, molecular weight, branching, concentration, or temperature which determine the resulting morphology (aggregates, precipitates, gels, crystals, etc.) and the crystalline type, when the substrate presents polymorphism.

Aqueous solutions of amylose and amylopectin, the two main constituents of starch, can also reorganize upon cooling[1,2] or addition of precipitant.[3,4] This behavior as well as the nature of the resulting structures, have a strong impact on properties of starch, like susceptibility to enzymatic hydrolysis or gel strength for example, in both food and non food applications. Amylopectin solutions usually yield B-type semicrystalline aggregates or gels.[5] Amylose can be recrystallized as lamellar,[3,15] fibrillar,[16,17] or spherulitic[10,12,18−19] crystals as well as polycrystalline powders[15] with the A or B allomorphic type observed in native starch granules depending on their botanical origin (for a review, see Buleon and co-workers[6]). The resulting morphology and allomorphic type depend on temperature, concentration, solvent, and degree of polymerization (DP) of the amylose chains.[7−12,3] High concentrations, high temperatures, and short chains are known to induce A-type crystallization, encountered mostly for native cereal starches. This has been observed when linear chains with well-defined DP, prepared following different procedures, were used. One consists of performing a mild acid hydrolysis of raw starch in order to isolate the crystalline fraction of the granules.[8,13−14] For instance, acid hydrolysis of potato starch during 48 h at 65 °C releases single-branched DP 21 chains.[8] Short amylose chains can also be obtained by enzymatically debranching glycogen which yields linear chains with a DP 11.[9] In vitro synthesis by phosphorylase is another way to produce α-glucan chains. According to Pfannemüller,[11] crystalline precipitates formed at room temperature from aqueous solutions gave the A-type for DP 10−12 and the B-type for DP 13 and above.

A polymorphic transition from B-type to A-type can also occur in specific conditions of temperature and hydration as shown for raw starch[20−23] or B-type "lintners",[24] prepared by mild acid hydrolysis of potato starch. Two possible mechanisms are suspected for this polymorphic transition, including either a reorganization of the double helices induced by the removal of water molecules from the B-type unit cell[25] or the melting of the B-type crystallites, which have a lower melting temperature,[26] followed by a recrystallization into the more stable A-type allomorph.[27]

Recently, Cerestar (Cargill) has developed and patented a new method to prepare a starch product which exhibits a substantial resistance to hydrolysis by α-amylases. The procedure is based on the debranching and recrystallization of maltodextrins at high concentration (25% w/v).[28] Maltodextrins are commercial products prepared by partial enzymatic hydrolysis of native starch. They consist of (i) short linear chains resulting from the hydrolysis of amylose or sidechains of amylopectin[29] and (ii) branched residues, released from the hydrolysis of the long chains between branching points within amylopectin clusters.[30] The resistant starch produced by debranching and crystallization of such maltodextrins has proved to be formed predominantly of A-type crystals aggregates with reduced accessibility to enzymes.[31] This study investigates the mechanisms involved in the debranching and crystallization of maltodextrins at high concentration and their impact on the resulting structures.

* To whom correspondence should be addressed. Fax: +33 240 61 50 43. E-mail: buleon@nantes.inra.fr.

[†] INRA.

[‡] Centre de Recherches sur les Macromolécules Végétales.

10.1021/bm049881i CCC: $27.50 © 2004 American Chemical Society
Published on Web 06/29/2004

2. Materials and Methods

Samples. The samples were prepared from maize maltodextrins (Cerestar, Vilvoorde, Belgium) according to a protocol derived from the method described in the EP-0846704A20 patent. 10 g of maltodextrins were solubilized in 30 mL of water at 95 °C during 1 h and cooled to 52 °C. The pH was adjusted to 4.0 ± 0.1 with 0.1 N HCl. 10 mg of isoamylase (Hayashibara Inc., Japan) and 10 mg of sodium benzoate were then added in order to initiate the debranching. The mixture was heated at 52 °C and stirred with a rotative blade.

The debranching rate was determined from 4 mL samples at 1 min and 1, 2.5, 4, 5, 6, and 8 h. Samples were put at 100 °C in a water bath during 15 min to inhibit the enzyme. They were finally dried under P_2O_5 until constant weight and smoothly milled in a mortar.

The rate of crystallization and resulting structure were determined from the precipitate: 4 mL were sampled at 12, 18, 24, 36, and 48 h and centrifuged at 52 °C during 10 min at 7000 tr min^{-1}. The morphology was immediately analyzed by transmission electron microscopy (TEM) and the allomorphic type determined by X-ray diffraction. The percentage of crystallinity was determined only after adjustment of the water content (see the X-ray diffraction analysis section). The molecular structure was studied after drying with P_2O_5 until constant weight and smooth milling in a mortar.

Molecular Analysis. Samples were solubilized in 1 M potassium hydroxyde (100 μL) during 2 days at 4 °C under gentle magnetic stirring and subsequently diluted with 900 μL of pure water. Resulting solutions were filtered through 0.45 μm or 5 μm sieves. Then, an aliquot was injected into a high-performance anion-exchange chromatograph with a pulsed amperometric detector system (HPAEC−PAD) or a high-pressure size exclusion chromatograph with multiple angle laser light scattering detection (HPSEC-MALLS). For analysis of residual branched materials still present in the precipitate, HPAEC profiles were compared before and after complete debranching by isoamylase.

Isoamylase Debranching. Samples (50 mg) were solubilized in 1 M potassium hydroxyde (1 mL) during 2 days at 4 °C under gentle magnetic stirring and subsequently diluted with 900 μL of pure water. 0.1 M HCl (250 μL) and citrate buffer (50 mM, pH 3.8) (500 μL) were added to 250 μL of this resulting solution. Debranching was performed on 800 μL by adding 10 μL of isoamylase and incubating 48 h at 37 °C in a water bath.

HPAEC/PAD Analysis. Samples were analyzed using HPAEC−PAD before and after isoamylase debranching. Samples were injected into a CarboPac PA-100 anion exchange column (250 mm × 4 mm) coupled to a CarboPac PA-100 guard column. The acetate gradient system included two eluents: 150 mM NaOH (eluent A) and 150 mM NaOH containing 600 mM NaOAc (eluent B). The flow rate was 1 mL min^{-1}. The elution gradient was (i) 0−5 min with 100% eluent A and (ii) 5−6 min with a linear gradient from 0% to 10% eluent B, 6−9 min with a second linear gradient from 10% to 25% eluent B, 9−24 min with a third linear gradient from 25% to 45% eluent B, 24−49 min with a fourth linear gradient from 45% to 57% eluent B, 49−61 min with a fifth linear gradient from 57% to 63% eluent B, 61−65 min with a linear gradient to 100% eluent B, 65−70 min with 100% eluent A, and finally 70−71 min with a linear gradient from 100% to 0% eluent B and 71−95 min with 100% eluent A. As in HPAEC−PAD, response coefficients decrease with increasing DP, % area of long chains are not representative of the exact weight fraction of each DP.

HPSEC/MALLS Analysis. The equipment was the same as that previously described[32] except for a Waters 590 programmable HPLC-pump and a Waters 717 autosampler. The SEC columns used were three hemabio (1000, 100 and 40) (250 mm × 8 mm) from Sopares (Gentilly, France) together with a hemabio guard column from Sopares, and the column and the precolumn were maintained at 40 °C using a Crococil temperature control from Cluzeau (Bordeaux, France). The two on-line detectors were a MALLS instrument, Dawn DSP-F, fitted with a K5 flow cell and a He−Ne laser, (λ = 632.8 nm), supplied by Wyatt Technology Corporation (Santa Barbara, CA) and an ERC-7515A refractometer from Erma (Tokyo, Japan). Before use, the mobile phase (Millipore water containing 0.1 N potassium hydroxyde) was carefully degassed and filtered through Durapore GV (0.2 μm) membranes from Millipore and eluted at a flow rate of 1 mL min^{-1}. A value of 0.146 mL g^{-1} was used as the refractive index increment (dn/dc) for the glucans. An interdetector delay volume of 195 μL was determined by injecting BSA-monomer. Normalization of the photodiodes was obtained using a low molar mass pullulan standard (P20).

X-ray Diffraction Analysis. X-ray diffraction (XRD) was performed either directly on fresh samples after centrifugation or after adjustment of water content to 17% H_2O (w.b.) for determination of the degree of crystallinity. This was performed by water sorption at 90% of relative humidity (RH) for 10 days under partial vacuum in the presence of a saturated baryum chloride solution. The samples (20 mg) were then sealed between two tape foils to prevent any significant change in water content during the measurement. Diffraction diagrams were recorded using an INEL (Artenay, France) spectrometer working at 40 kV and 30 mA operating in the Debye−Scherrer transmission mode. The X-ray radiation Cu Kα_1 (λ = 0.15405 nm) was selected with a quartz monochromator. Diffraction diagrams were recorded during 2 h exposure periods, with a curve position sensitive detector (INEL CPS 120). The relative crystallinity was determined after normalization of all recorded diagrams at the same integrated scattering between 3 and 30° (2θ). A- and B-type recrystallized amyloses were used as crystalline standards, after scaled subtraction of an experimental amorphous curve in order to get nul intensity in the regions without diffraction peaks. Dry extruded potato starch was used as the amorphous standard.

The degree of crystallinity of samples having a pure allomorphic type was determined using the method initially developped by Wakelin and co-workers[33] for cellulose. The percentage of crystallinity was taken as the slope of the line $(I_{sample} - I_{amor})_{2\theta} = f(I_{crys} - I_{amor})_{2\theta}$ where I_{sample}, I_{amor}, and

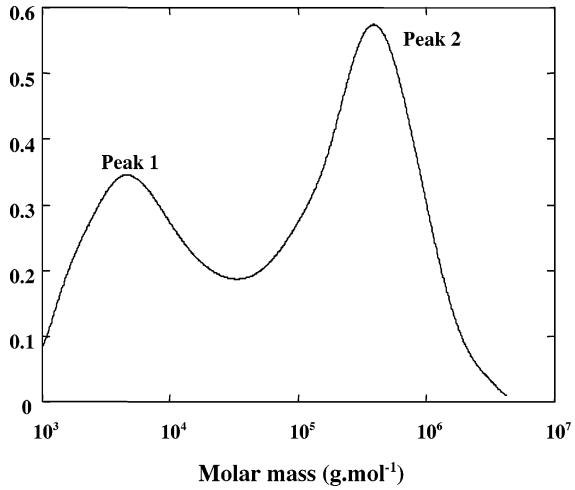

Figure 1. Molecular weight distribution of maltodextrins before debranching.

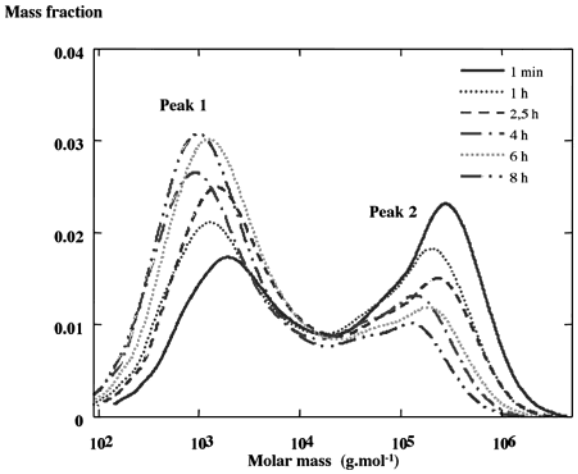

Figure 2. Molecular weight distribution of maltodextrins at different debranching times.

I_{crys} are the diffracted intensity of the sample, the amorphous, and the crystalline standards, respectively.

For substrates presenting both A- and B-type structures, another method was used. The diffraction diagram was considered as a linear combination of amorphous and crystalline (A- and B-type) standards diagrams. A multilinear regression was used to fit the experimental diagram and therefore to determine the respective fractions of A-type, B-type, and amorphous phases. The resulting percentage of crystallinity was then confirmed with Wakelin's method using a crystalline standard diagram built from the calculated proportions of A- and B-type.

Transmission Electron Microscopy. A drop of precipitate in suspension was deposited on glow-discharged carbon-coated microscopy grids. The liquid in excess was blotted with filter paper, and a drop of 2% uranyl acetate negative stain was added prior to drying. The stain in excess was blotted, and the remaining thin liquid film was allowed to dry. Unstained specimens were also prepared and equilibrated overnight in a 95% r.h. atmosphere. Once mounted in a Gatan 626 cryoholder, they were quench-frozen in liquid nitrogen, transferred to the microscope and observed at low temperature (−180 °C). As described elsewhere in detail,[34,35] cryo-TEM specimens were prepared by quench-freezing thin liquid films of the suspensions into liquid ethane using a Leica EMCPC device. The specimens were then mounted onto the Gatan 626 holder previously cooled to −180 °C by liquid nitrogen. All samples were observed in low dose conditions, using a Philips CM 200 "Cryo" microscope operated at 80 kV for conventional imaging and 200 kV for diffraction purpose. Micrographs were recorded on Kodak SO163 films.

3. Results

Effect of Debranching on the Molecular Weight Distribution of Maltodextrins. The molecular weight distribution (MWD) of maltodextrins before debranching, obtained by HPSEC/MALLS, is given in Figure 1. The MWD presents 2 peaks centered at about 1×10^3 g mol^{-1} (DP 12) and 2.8×10^5 g mol^{-1} (DP 1700) respectively named peaks 1 and 2. The variation of MWD with the debranching time is shown in Figure 2. Debranching of maltodextrins started very rapidly as an important change to lower DP was observed after only 1 h. Moreover, no further significant action of isoamylase was detected between 6 and 8 h. From 1 min to 8 h, the position of peaks 1 and 2 shifted from DP 12 to 6 and from DP 1700 to 800, respectively. In the same time, the surface ratio of peak 1 to peak 2 increased from 0.8 to 3.2.

Table 1. Amount of Precipitated Maltodextrins as a Function of Incubation Time

time (h)	12	18	24	36	48
fraction of precipitated dextrins (%)	25 ± 4	34 ± 4	47 ± 4	85 ± 4	100

Therefore, in Figure 1, peak 1 corresponds to fragments of amylose and short chains of clusters released by α-amylolysis during the production of maltodextrins, whereas peak 2 is assigned to residues of clusters (branched chains) as well as longer amylose fragments (linear chains). The debranching of clusters (Figure 2) led to a decrease of peak 2 and an increase of peak 1 (short chains released by isoamylase). As reported by Bertoft,[30] the α-amylolysis of amylopectin is known to induce hydrolysis of the long chains between branching points thus releasing clusters. When the treatment is extended, many short chains corresponding to the hydrolysis of the external chains are also released.[29]

Precipitation and Crystallization of Debranched Maltodextrins. *Amount of Precipitated Maltodextrins.* After 12 h of debranching, a precipitate corresponding to 25% of the total initial mass of maltodextrins was recovered. Then precipitation/crystallization gradually occurred up to 48 h when all chains had precipitated. The amount of precipitated product as a function of incubation time is given in Table 1.

Crystalline Structure versus Incubation Time. X-ray diffraction diagrams of the precipitate formed at different times of incubation are presented in Figure 3. The corresponding degree of crystallinity and allomorphic composition are given in Table 2. The crystallinity increases from 29 to 72% between 12 and 48 h, whereas a gradual shift from almost pure B-type to pure A-type structure is simultaneously observed.

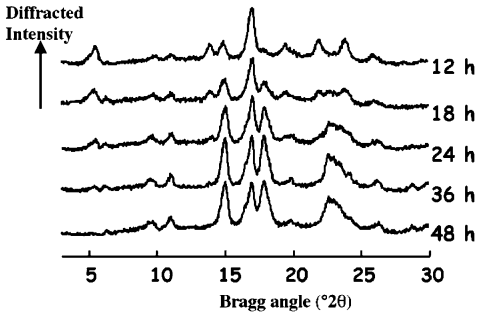

Figure 3. X-ray diffraction spectra of the precipitates formed at different incubation times.

Table 2. Degree of Crystallinity and Allomorphic Composition as a Function of Incubation Time

incubation time	crystallinity (%)	A-type structure (%)	B-type structure (%)
12 h	29 (±3)	13 (±5)	87 (±5)
18 h	37 (±3)	47 (±5)	53 (±5)
24 h	58 (±3)	79 (±5)	21 (±5)
36 h	78 (±3)	85 (±5)	15 (±5)
48 h	72 (±3)	100 (±5)	0

Crystallization Mechanism. The gradual transition from B- to A-type may result from two phenomena. Either there is a polymorphic change from the precipitated B-type structure into the A-type, as observed for starchy samples in specific conditions of temperature and hydration,[23,24] or the crystalline residue appearing at times above 12 h is strictly of A-type. In this case, the relative fraction of B-type allomorph in the final product is small and hardly detectable by XRD.

The first hypothesis was ruled out by allowing the B-type product recovered by centrifugation after 12 h of incubation to be kept at 52 °C for 48 h in the same conditions of concentration as during incubation. In these conditions, no B to A transition was evidenced.

The second hypothesis was validated by calculating the B-type fraction in the final product taking into account the respective amount precipitated at 12 and 48 h and the corresponding degree of crystallinity. It was estimated to 7% which is below the XRD detection threshold for such substrates. Indeed, a very small peak at $2\theta = 5.6°$ and a very weak shoulder at $2\theta = 24°$ are visible on the diffraction diagram of the final product in Figure 3 but their intensity were too low to yield any contribution to the calculation of B to A ratio. Moreover, it was checked that no further B-type crystallization occurred after 12 h since the further incubation for 48 h at 52 °C of the corresponding supernatant only led to A-type crystallization.

Therefore, the shift from a global B-type crystallinity to a global A-type crystallinity was attributed to a split crystallization with a preferential B-type crystallization during the first 12 h of incubation, followed by A-type crystallization between 12 and 48 h.

Molecular Weight Distribution of the Precipitate Formed at Different Incubation Times. The MWD of the products precipitated at 12 (RS-12) and 48 h (RS-48) of incubation are shown in Figure 4. They are bimodal and present a high polydispersity, with peaks ranging from a few monomers to

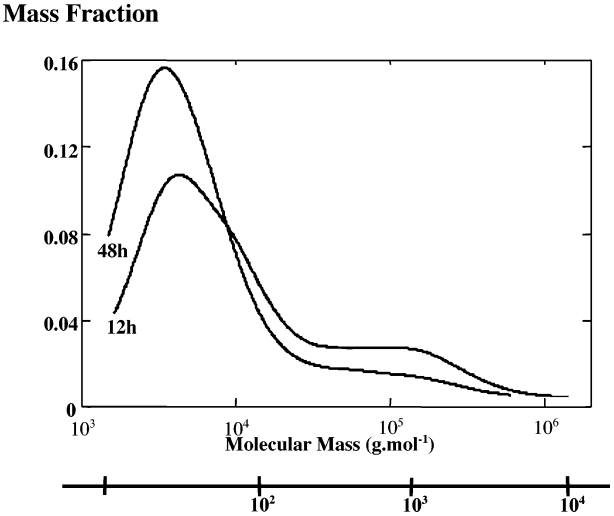

Figure 4. Molecular weight distribution of RS-12 and RS-48.

Table 3. Molecular Weight Distribution of RS-12 and RS-48

	incubation time			
	12 h		48 h	
	peak 1	peak 2	peak 1	peak 2
peak area (%)	86.3	13.7	95.0	5.0
$\overline{DP}_{max}$	27.2		22.7	
$\overline{DP}_n$	31.2	713	24.1	597
$\overline{DP}_w$	63.8	1239	42.0	970

DP 250 and from DP 250 to DP 6×10^3 respectively. The first distribution (i.e., the shorter chains) represents 86 and 95% of the precipitates at 12 and 48 h respectively, whereas the corresponding DP decreases from 31.2 to 24.1 (Table 3).

To determine the characteristics of the chains precipitated at 12 h and between 12 and 48 h respectively, the first fraction (named F-12) was isolated by centrifugation. A second fraction was obtained by keeping the supernatant at 52 °C during an additional 36 h and centrifugation the resulting residue (named F-48). The corresponding MWD was studied by HPAEC−PAD. A typical result is shown in Figure 5 for the F-48 sample. Chromatograms contain well resolved peaks corresponding to chains with DP < 50 and a single broader peak centered at the elution volume of the pure eluent ($V_{acetate}$) and corresponding to the chains with DP > 50. A subsequent complete debranching was performed in order to check if some branched chains were still present after incubation. For F-12, the peak corresponding to DP > 50 represents 20% and 13% of total chromatogram area, before and after complete debranching, respectively. Therefore, the percentage of long linear chains and branched chains could be estimated to 13% and 7%, respectively. The corresponding values for F-48 were estimated to 1% and 5%, respectively. Consequently, most long linear chains were present in F-12 and were probably involved in the corresponding B-type structure. This extensive study by HPAEC also shows that branched molecules were still present after 12 h of incubation.

Morphology of the Insoluble Products. The morphology of the insoluble fractions obtained after 12 and 48 h was studied by TEM. Figure 6a shows a preparation from

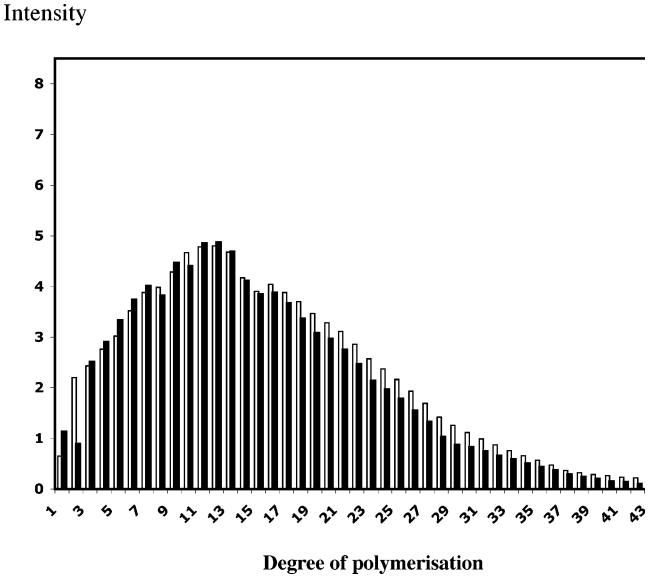

Figure 5. HPAEC−PAD analysis of the chain length distribution of F-48 sample before (■) and after (□) complete debranching.

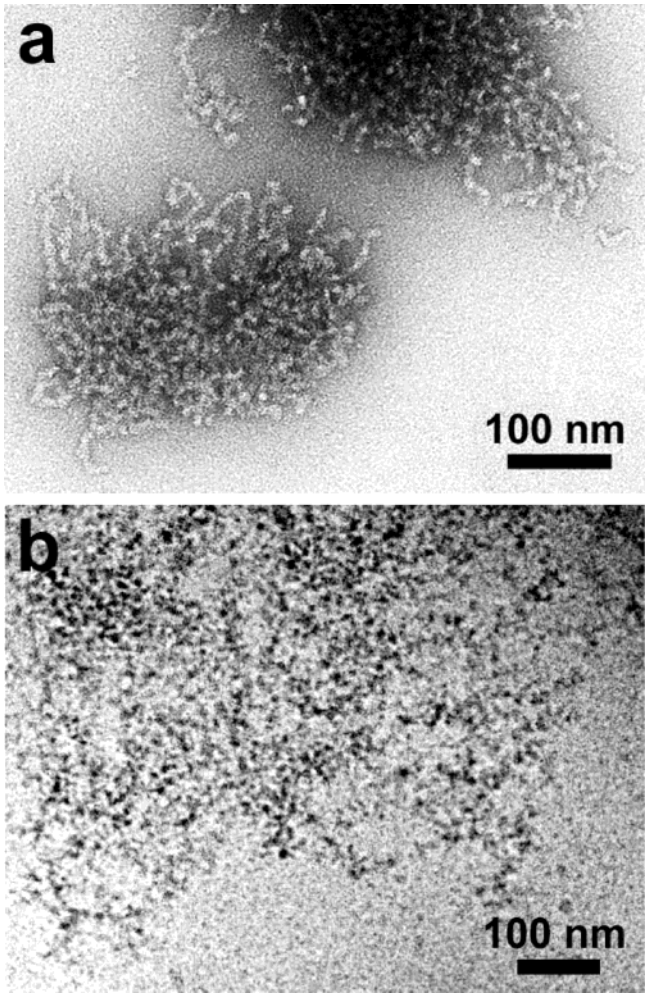

Figure 6. TEM images of networks observed in the insoluble product obtained after 12 h. (a) The sample has been negatively stained with uranyl acetate. (b) An unstained network is seen embedded in a thin film of vitreous ice.

RS-12 after negative staining. The sample appears to be composed of loose networks, consisting of wormlike objects with a 9−11 nm width. Larger compact aggregates were also

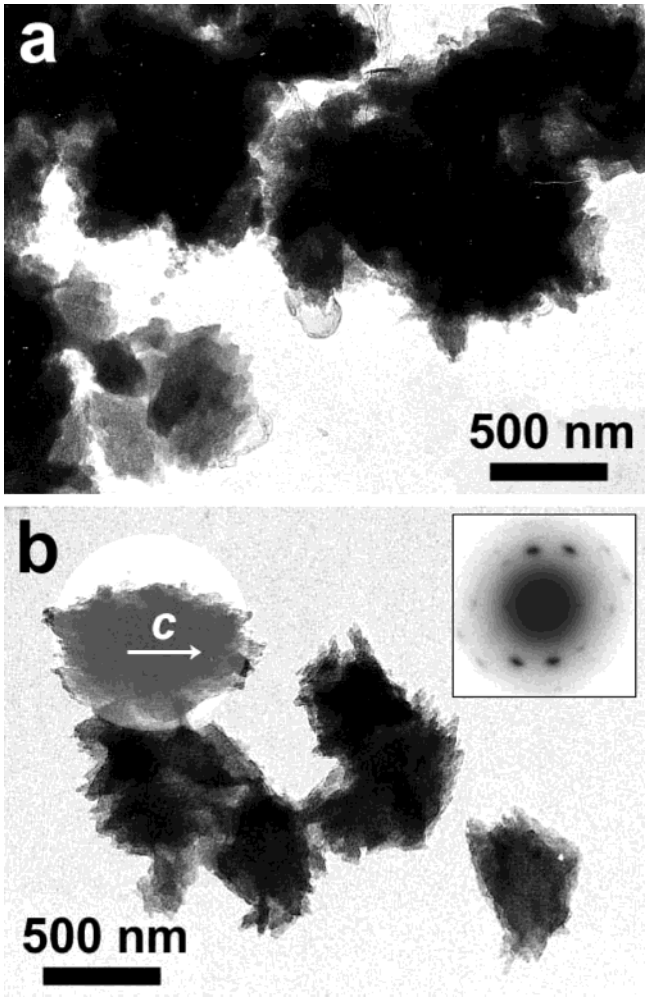

Figure 7. (a and b) TEM images of unstained frozen-hydrated samples from the insoluble product obtained after 48 h. Insert in (b) electron diffraction pattern recorded from the circled aggregate. The chain axis *c* of the crystal structure is indicated.

observed (not shown) and assumed to correspond to the 13% of A-type structures detected after 12 h of incubation. To check that the networks were not due to a reprecipitation phenomenon (also called "retrogradation"[35]) that would have occurred during the cooling following the preparation of the grid, a cryo-TEM sample was prepared by quench-freezing a thin film of the hot suspension. Figure 6b shows a network embedded in vitreous ice, thus confirming the existence of the networks in the incubation media at 52 °C. TEM images of the insoluble fractions isolated at 18 and 24 h showed a gradual increase of the amount of crystalline aggregates to the detriment of the networks present at 12 h. No networks were observed in preparations from RS-48.

A typical TEM image of a frozen-hydrated preparation from RS-48 is presented in Figure 7. It consists of more or less ovoidal aggregates approximately 700−800 nm long and 200−300 nm wide. Judging by the appearance of the thinner objects, the aggregates seem to be stacks of individual platelets with a length ranging between 50 and 100 nm. Electron diffraction patterns were recorded from individual aggregates. An example is shown in Figure 7b. The diffraction pattern of the composite aggregate is unique and corresponds to A-type crystals with a chain axis oriented along the aggregate longer dimension. That means that the

constitutive elementary platelets have a similar orientation. A detailed structural study of this product, using TEM and comparison to model A-type amylose crystals with similar diffraction patterns, was recently conducted in order to determine the structural parameters responsible for the unusually high resistance of these aggregates to α-amylase.[31] We concluded that RS-48 consists of aggregates of A-type platelet crystals that epitaxially grew on each other, limiting the accessibility of double helices to the enzymes.[31]

4. Discussion

The crystallization behavior of debranched maize starch maltodextrins at 52 °C and at high concentration (25% w/v) was studied by analysis of MWD, crystallinity, and morphology of samples precipitated at different times of incubation. A split crystallization was evidenced that involves, in a first stage, the aggregation of the longer linear or branched chains into B-type networks, followed by the precipitation of the shorter linear chains into dense aggregates of A-type crystals. Such a split crystallization that depends on the molecular weight is well-known for synthetic polymers.[36] It is commonly used for their fractionation, by cooling of solutions at successive temperature steps. A similar dependence of the solubilization temperature on the molecular weight has also been demonstrated for amylose.[26]

The results obtained on the relationship between the molecular structure and the precipitation rate, the resulting morphology, or the crystalline type are consistent with the data existing in the literature for crystallization of starchy substrates. High temperatures and short chains are known to favor A-type crystallization,[3,7,9,11,13] whereas B-type gels or aggregates are formed at lower temperature with higher molecular weight molecules. It is remarkable that such a general behavior is retained in the complex and concentrated mixture studied here. The time necessary for the complete precipitation of debranched maltodextrins is long (48 h), due to the small average chain length, the temperature used (52 °C), and the absence of precipitant.

The branched networks formed after 12 h are similar to those observed by TEM on samples obtained by reprecipitation of solutions of α-glucan chains. It was reported for solutions retrograded at 30 °C,[37] for 2% to 8% (w/v) amylose gels observed after cryo-fracture and surface replication,[1] and more recently for retrograded dilute solutions of amylose and amylopectin observed by cryo-TEM.[35] Moreover, the A-type platelets constituting the RS-48 aggregates resemble the A-type amylose single crystals obtained by crystallizing DP 15 amylose chains in the presence of ethanol at 50 °C[3] or acetone at 55−60 °C.[15,31] They are obtained here at almost the same temperature without adding any precipitant, due to the high concentration used (25%). However, in such conditions, their complete precipitation takes 48 h.

The aggregates in RS-48 also yield electron diffraction patterns similar to those of low DP recrystallized A-type crystals. Therefore, it appears that the maltodextrins chains released by isoamylase debranching behave in a standard way upon crystallization, even at this high concentration. The longer chains aggregate early on due to their lower solubility and form networks, whereas short linear chains precipitate in aggregates of crystals similar to those obtained from recrystallized linear fractions with DP 15−30. Moreover, the temperature corresponds to that usually used for the formation of A-type crystals from amylose solutions.[3,15]

5. Conclusions

The debranching action of isoamylase on concentrated solutions of starch maltodextrins and their crystallization behavior was studied for the first time. The mechanisms involved at the different stages of the process were investigated through the analysis of molecular weight distribution, crystallinity, and morphology of the corresponding insoluble products. The factors influencing the split crystallization and the characteristics of the products formed at different stages were determined. The conditions used at the laboratory scale were very close to those applied in the industrial process used to prepare resistant starch and patented by Cerestar (Cargill). Some structural factors such as the epitaxial aggregation of crystalline platelets yielding a very low accessibility to α-amylase have been shown to be responsible for the resistance of the 48 h product.[31] The loose B-type network formed at 12 h is poorly crystalline, very accessible to α-amylase, and consequently more susceptible to enzymatic hydrolysis. This knowledge could be used to produce a range of products with a varying resistance to α-amylases, depending on the incubation time, temperature, and concentration. More generally, the control of the precipitation behavior at high concentration of polymeric chains originated from starch transformation could be used to optimize many starch-based products in both food and nonfood applications.

Acknowledgment. This work was funded by Cerestar, a Cargill company. The authors are grateful to B. Pontoire and M.P. Pacouret for technical assistance and to B. Kettlitz and J. Coppin (Cerestar) for helping to downsize the RS process at the laboratory scale.

References and Notes

(1) Leloup, V. M.; Colonna, P.; Ring, S. G.; Roberts, K.; Wells, B. *Carbohydr. Polym.* **1992**, *18*, 189−197.
(2) Gidley, M. J. *Macromolecules* **1989**, *22*, 351−358.
(3) Buleon, A.; Duprat, F.; Booy, F. P.; Chanzy, H. *Carbohydr. Polym.* **1984**, *4*, 161−173.
(4) Brisson, J.; Chanzy, H.; Winter, W. *Int. J. Biol. Macromol.* **1991**, *13*, 31−39.
(5) Ring, S. G.; Colonna, P.; l'Anson, K. J.; Kalichevsky, M. T.; Miles, M. J.; Morris, V. J.; Orford, P. D. *Carbohydr. Res.* **1987**, *162*, 277−293.
(6) Buleon, A.; Colonna P.; Planchot, V.; Ball, S. *Int. J. Biol. Macromol.* **1998**, *23*, 85−112.
(7) Hizukuri, S. *Agric. Biol. Chem.* **1961**, *25*, 45−49.
(8) Hizukuri, S.; Kaneko, T.; Takeda, Y. *Biochim. Biophys. Acta* **1983**, *760*, 188−191.
(9) Gidley, M. J.; Bulpin, P. V. *Carbohydr. Res.* **1987**, *161*, 291−300.
(10) Ring, S. G.; Miles, M. J.; Morris, V. J.; Turner, R.; Colonna, P. *Int. J. Biol. Macromol.* **1987**, *9*, 158−160.
(11) Pfannemüller, B. *Int. J. Biol. Macromol.* **1987**, *9*, 105−108.
(12) Planchot, V.; Colonna, P.; Buleon, A. *Carbohydr. Res.* **1997**, *298*, 319−326.
(13) Hizukuri, S.; Takeda, Y.; Usami, S.; Takase, Y. *Carbohydr. Res.* **1980**, *83*, 193−199.
(14) Putaux, J. L.; Molina-Boisseau, S.; Momaur, T.; Dufresne, A. *Biomacromolecules* **2003**, *4* (5), 1198−1202.
(15) Imberty, A.; Chanzy, H.; Perez, S.; Buleon, A.; Tran, V. *J. Mol. Biol.* **1988**, *201*, 365−378.

(16) Wu, H. C. H.; Sarko, A. *Carbohydr. Res.* **1978**, *61*, 7−25.
(17) Wu, H. C. H.; Sarko, A. *Carbohydr. Res.* **1978**, *61*, 27−40.
(18) Williamson, G.; Belshaw, N. J.; Self, D. J.; Noel, T. R.; Ring, S. G.; Cairns, P.; Morris, V. J.; Clark, S. A.; Parker, M. L. *Carbohydr. Polym.* **1992**, *18*, 179−187.
(19) Helbert, W.; Chanzy, H.; Planchot, V.; Buleon, A.; Colonna, P. *Int. J. Biol. Macromol.* **1993**, *15*, 183−187.
(20) Zobel, H. F. *Starch/Stärke* **1988**, *40*, 1−7.
(21) Stute, R. *Starch/Stärke* **1992**, *44*, 205−214.
(22) Lim, S. T.; Chang, E. H.; Chung, H. J. *Carbohydr. Polym.* **2001**, *46*, 107−115.
(23) Hoover, R.; Vasanthan, T. *Carbohydr. Res.* **1994**, *252*, 33−53.
(24) Le Bail, P.; Bizot, H.; Buleon, A. *Carbohydr. Polym.* **1993**, *21*, 99−104.
(25) Imberty, A.; Buleon, A.; Tran, V.; Perez, S. *Starch/Stärke* **1991**, *43*, 375−384.
(26) Moates, G. K.; Noel, T. R.; Parker, R.; Ring, S. G. *Carbohydr. Res.* **1997**, *298*, 327−333.
(27) Buleon, A.; Le Bail, P.; Colonna, P.; Bizot, H. In *The properties of water in foods−ISOPOW 6*; Reid, D. S., Ed.; Blackie Academic and Professional: London, 1998; pp 160−178.
(28) Kettlitz, B. W.; Coppin, J. V.; Roper, H. W.; Bornet, F. EP-0846704A2, 1996.
(29) Bertoft, E. *Carbohydr. Res.* **1989**, *189*, 181−193.
(30) Bertoft, E. *Carbohydr. Res.* **1986**, *149*, 379−387.
(31) Pohu, A.; Putaux, J.-L.; Planchot, V.; Colonna, P.; Buleon, A. *Biomacromolecules* **2004**, *5* (1), 119−125.
(32) Roger, P.; Colonna, P. *Int. J. Biol. Macromol.* **1996**, *19*, 51−61.
(33) Wakelin, J. H.; Virgin, H. S.; Crystal, E. *J. Appl. Phys.* **1959**, *30*, 1654−1662.
(34) Putaux, J. L.; Buleon, A.; Borsali, R.; Chanzy, H. *Int J. Biol. Macromol.* **1999**, *26*, 145−150.
(35) Putaux, J. L.; Buleon, A.; Chanzy, H. *Macromolecules* **2000**, *33*, 6416−6422.
(36) Flory, P. J. In *Principles of polymer chemistry*; Cornell University Press: Ithaca, NY, 1953.
(37) Harada, T.; Kanzawa, Y.; Kanenaga, K.; Koreeda, A.; Harada, A. *Food Struct.* **1991**, *10*, 1−18.

BM049881I